Structure
Article

Crystal Structure of Human Nicotinamide Riboside Kinase

Javed A. Khan,[1,2,3] Song Xiang,[1,3] and Liang Tong[1,*]
[1] Department of Biological Sciences, Columbia University, New York, NY 10027, USA
[2] Present address: Research and Development, Bristol-Myers Squibb, Princeton, NJ 08540, USA.
[3] These authors contributed equally to this work.
*Correspondence: ltong@columbia.edu
DOI 10.1016/j.str.2007.06.017

SUMMARY

Nicotinamide riboside kinase (NRK) has an important role in the biosynthesis of NAD$^+$ as well as the activation of tiazofurin and other NR analogs for anticancer therapy. NRK belongs to the deoxynucleoside kinase and nucleoside monophosphate (NMP) kinase superfamily, although the degree of sequence conservation is very low. We report here the crystal structures of human NRK1 in a binary complex with the reaction product nicotinamide mononucleotide (NMN) at 1.5 Å resolution and in a ternary complex with ADP and tiazofurin at 2.7 Å resolution. The active site is located in a groove between the central parallel β sheet core and the LID and NMP-binding domains. The hydroxyl groups on the ribose of NR are recognized by Asp56 and Arg129, and Asp36 is the general base of the enzyme. Mutation of residues in the active site can abolish the catalytic activity of the enzyme, confirming the structural observations.

INTRODUCTION

Nicotinamide adenine dinucleotide (NAD$^+$) is well known as a coenzyme in oxidation/reduction reactions. NAD$^+$ also serves as a substrate in several biochemical reactions, including ADP ribosylation, protein deacetylation, and ADP-ribose cyclization, which have important effects on genome stability, aging, calcium signaling, and other cellular processes (Berger et al., 2004; Blander and Guarente, 2004; Denu, 2005; Guse, 2005; Khan et al., 2007; Lee, 2004; Li et al., 2006; Magni et al., 1999, 2004a; Revollo et al., 2007; Schreiber et al., 2006; Ying, 2006). NAD$^+$ donates its ADP-ribosyl group in these reactions. As a result, the glycosidic bond between the nicotinamide group and the ribose is broken, and the NAD$^+$ molecule is destroyed. NAD$^+$ biosynthesis is therefore crucial in cells that undergo rapid turnover of this molecule. For example, inhibition of NAD$^+$ biosynthesis in cancer cells can lead to a decrease in cellular NAD$^+$ levels, ultimately causing apoptosis (Hasmann and Schemainda, 2003; Khan et al., 2006).

Several different pathways are known for NAD$^+$ biosynthesis (Khan et al., 2007; Magni et al., 1999, 2004a; Rongvaux et al., 2003). The de novo pathway produces NAD$^+$ from tryptophan in most eukaryotes, whereas the salvage pathways produce NAD$^+$ from nicotinic acid (NA) or nicotinamide. NA is generally acquired from the diet or from the hydrolysis of nicotinamide, whereas nicotinamide is the breakdown product of NAD$^+$. The compounds NA and nicotinamide are first converted to their mononucleotide forms (NAMN or NMN), and then the enzyme NA/nicotinamide adenylyltransferase (NMNAT) produces the dinucleotides (NAAD$^+$ or NAD$^+$) (Magni et al., 2004b). NAAD$^+$ is converted to NAD$^+$ by the enzyme NAD$^+$ synthetase (Jauch et al., 2005; Rizzi et al., 1996; Wojcik et al., 2006).

Recently, a fourth pathway of NAD$^+$ biosynthesis that uses nicotinamide riboside (NR) as the starting point was characterized (Bieganowski and Brenner, 2004). The enzyme nicotinamide riboside kinase (NRK) catalyzes the phosphorylation of NR to produce NMN (Figure 1A), which can then be converted to NAD$^+$ by NMNAT. NRK is also the enzyme responsible for the activation of tiazofurin (Figure 1B) and several other anticancer agents (Bieganowski and Brenner, 2004). These compounds are ultimately converted to NAD$^+$ analogs, and their clinical effects are derived from inhibition of inosine mononucleotide dehydrogenase, the rate-limiting enzyme in guanine nucleotide biosynthesis (Grifantini, 2000; Jager et al., 2002; Pankiwicz et al., 2004). Therefore, besides its role in NAD$^+$ metabolism, NRK is also an important enzyme in anticancer therapy.

NRK is found in most eukaryotes, from yeast to humans. There are two isoforms of this enzyme in humans, NRK1 and NRK2. The amino acid sequences of these enzymes are highly conserved (Figure 1C). They belong to the deoxynucleoside kinase (dNK) superfamily (Eriksson et al., 2002), although the sequence conservation is very low (less than 20% identity). Weak sequence homology is also recognized with the nucleoside monophosphate kinase (NMP kinase) superfamily (Yan and Tsai, 1999). Currently, no structural information is available on any of the NRKs. We report here the crystal structures of human NRK1 in a binary complex with the product NMN at 1.5 Å resolution and in a ternary complex with tiazofurin and ADP at 2.7 Å resolution.

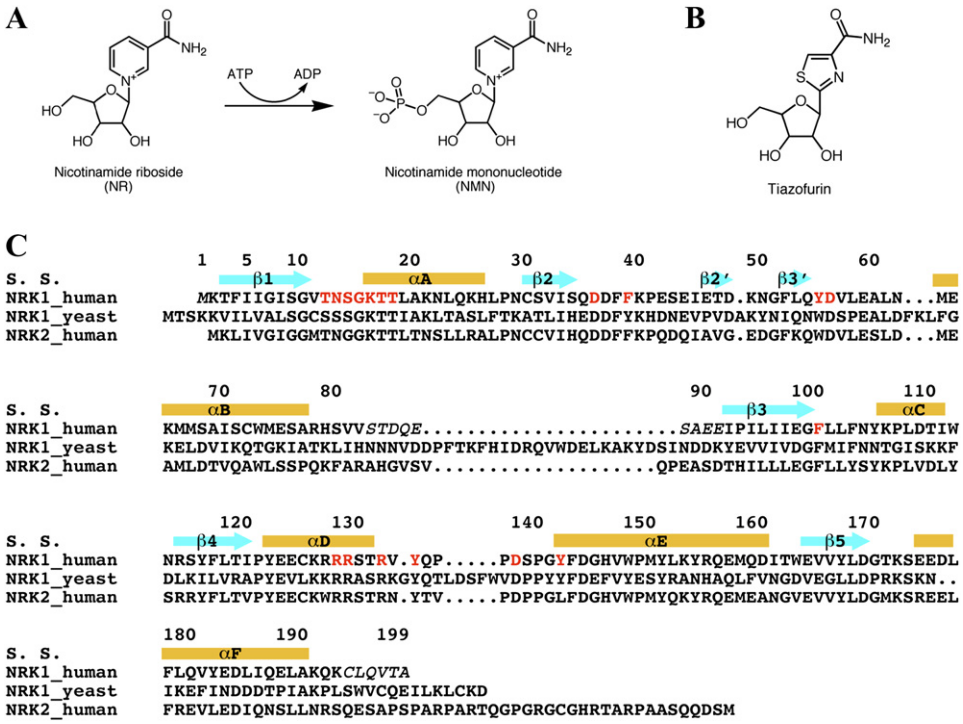

Figure 1. Sequence Alignment of Nicotinamide Riboside Kinases

(A) The chemical reaction catalyzed by nicotinamide riboside kinases (NRKs).

(B) The chemical structure of tiazofurin.

(C) Sequence alignment of human NRK1 (SwissProt entry Q9NWW6), NRK2 (Q9NPI5), and yeast (*S. cerevisiae*) NRK1 (P53915). The secondary-structure elements are labeled. Residues shown in red are involved in substrate binding and/or catalysis. Residues in italics are disordered in the current structure. A dot represents a deletion.

RESULTS AND DISCUSSION

Overall Structure of Human NRK1

The crystal structure of human NRK1 in complex with the reaction product NMN has been determined at 1.5 Å resolution by the selenomethionyl single-wavelength anomalous diffraction (SAD) method (Hendrickson, 1991). The crystal structure of NRK1 in a ternary complex with ADP and the anticancer drug tiazofurin has been determined at 2.7 Å resolution. The refined structures have excellent agreement with the crystallographic data and the expected bond lengths, bond angles, and other geometric parameters (Table 1). The majority of the residues (90%) are in the most favored region of the Ramachandran plot, and none of the residues are in the disallowed region.

The current refined model for the NMN complex contains residues 2–82 and 92–193 of NRK1 (Figure 2A), and that for the ADP:tiazofurin complex contains residues 2–79 and 92–192 (Figure 2B). No electron density was observed for residues 83–91 and those at the C terminus of the recombinant protein (including the hexahistidine tag). These residues are probably disordered in the crystals. They correspond to regions of poor sequence conservation among these proteins (Figure 1C). In fact, yeast NRK1 has an insertion of more than 20 residues in the region between residues 83 and 91 of human NRK1.

The structure of NRK1 contains a central, five-stranded parallel β sheet (strands β1–β5), with five α helices on both faces (Figure 2A). There are two inserts to the central α/β/α core of the structure. One is in the connection between strand β2 and helix αB and contains a small β hairpin (strands β2′ and β3′). The other insert is in the connection between β4 and αE and contains a helix (αD). Both inserts are located at the C-terminal end (referred to as the top, Figure 2A) of the parallel β sheet in the core and help form the active site of the enzyme (see below).

The missing segment (residues 83–91) corresponds to the loop connecting helix αB and strand β3 and is located at the bottom of the β sheet, far away from the active site (Figure 2A).

Structural Conservation with Other Kinases

Comparisons with structures in the Protein Data Bank, by using the program Dali (Holm and Sander, 1993), show that NRK1 shares significant structural similarity (*Z* score of 9-15) with a large number of kinases, including members of the dNK superfamily (Figure 3A) (Eriksson et al., 2002; Welin et al., 2007), the NMP kinase superfamily (adenylate kinase, guanylate kinase, UMP kinase) (Figure 3B) (Abele and Schulz, 1995; Appleby et al., 2005; Stehle and Schulz, 1992; Yan and Tsai, 1999), gluconate kinase (Kraft et al., 2002), shikimate kinase (Hartmann et al., 2006), thymidylate kinase (Lavie et al., 1998a, 1998b), panthothenate

Table 1. Summary of Crystallographic Information

Ligands	NMN	ADP + Tiazofurin
Space group	$C222_1$	$P2_1$
Number of unique NRK1 molecules	1	16
Maximum resolution (Å)	1.5	2.7
Number of observations	455,572	366,557
Number of reflections[a]	74,763	116,539
R_{merge} (%)[b]	8.7 (46.2)	9.5 (28.0)
I/σI	23.3 (2.8)	13.2 (3.0)
Resolution range used for refinement (Å)	30–1.5	30–2.7
Completeness (%)	100 (99)	95 (74)
R factor (%)[c]	19.1 (26.9)	20.7 (30.3)
R_{free} (%)	20.6 (27.8)	23.5 (32.8)
Rms deviation in bond lengths (Å)	0.004	0.010
Rms deviation in bond angles (°)	1.2	1.5
PDB accession code	2QG6	2QL6

[a] The number for the selenomethionyl protein includes both Friedel pairs.
[b] $R_{merge} = \sum_h \sum_i |I_{hi} - \langle I_h \rangle| / \sum_h \sum_i I_{hi}$. The numbers in parentheses are for the highest-resolution shell.
[c] $R = \sum_h |F_h^o - F_h^c| / \sum_h F_h^o$.

kinase (Yun et al., 2000), and chloramphenicol phosphotransferase (Izard and Ellis, 2000). However, the sequence conservation between NRK1 and these other enzymes is very low, in the 13%–20% range for structurally equivalent residues.

The overall structures of these enzymes contain a central, five-stranded parallel β sheet, and the active site is located at the top of this sheet. The two inserts in the structures provide crucial residues for substrate recognition and catalysis. Specifically, ATP is bound between the second insert (known as the LID) and the core of the enzyme (Figure 3B), whereas the phospho-acceptor substrate is bound between the LID and the first insert (Figure 3B), also known as the NMP-binding domain.

In most of these structures, the LID contains a helix followed by a loop. Two Arg residues, corresponding to Arg128 and Arg132 in NRK1, are highly conserved in this region(Figure 1C). The former is important for binding the adenine base of ATP (Figure 3B), whereas the latter is important for binding the phosphate groups.

In comparison, the structure of the NMP-binding domain is highly divergent among these structures (Figures 2A, 3A, and 3B), reflecting the fact that these enzymes phosphorylate a diverse set of (small-molecule) substrates. In fact, the small β hairpin structure appears to be unique to NRK1.

Binding Mode of NMN and Tiazofurin

The reaction product NMN is bound in a pocket formed by residues in the LID and NMP-binding domains, with only minor contributions from residues in the core (Figure 4A). Both hydroxyl groups on the ribose are recognized by direct hydrogen-bonding interactions to the side chains of Asp56 and Arg129, and the latter residue also has ion-pair interactions with the side chain of Asp138. The phosphate group is recognized by ionic interactions with the side chain of Arg132 as well as hydrogen-bonding interactions with the side chains of Thr12, Lys16 (in the P loop), and Tyr134 (Figure 4A).

The nicotinamide group is surrounded by three aromatic side chains (Phe39, Tyr55, and Tyr134) and by Pro136. However, the electron density for this group is rather weak based on the crystallographic analysis, and the amide group is projected toward the solvent and is not directly recognized by the enzyme (Figure 4B). The binding mode of this ring is defined more clearly in the structure of the ternary complex with ADP:tiazofurin (Figure 4C). The structural analysis confirms that tiazofurin is a substrate mimic and has essentially the same binding mode as the NR portion of NMN (Figure 4A). The lack of specific recognition of the nicotinamide ring is consistent with biochemical data showing that NRK can phosphorylate other pyrimidine and purine nucleoside substrates (Bieganowski and Brenner, 2004; Sasiak and Saunders, 1996). NRKs could also play an important role in the biosynthesis of these NMPs.

The structure shows that the 5′ hydroxyl group of the ribose in tiazofurin is hydrogen bonded to the side chain of Asp36 (Figure 4A), suggesting that this residue could be the general base that deprotonates the hydroxyl group for catalysis (see below). An acidic side chain is the general base for most members of the dNK and NMP kinase superfamilies of enzymes (Eriksson et al., 2002; Yan and Tsai, 1999).

Binding Mode of ADP

Clear electron density was observed for the ADP molecule based on the crystallographic analysis (Figure 5A). The β-phosphate group interacts with the P loop, 10-GVTNS GKTT-18, linking strand β1 and helix αA (Figure 5B). One of the terminal oxygen atoms on the α-phosphate group is hydrogen bonded to the side chain of Thr18, which is also conserved among many members of this superfamily of enzymes (Figure 1C). In the structure of the NMN complex, a phosphate group is bound in a similar position to that of the β-phosphate of ADP (Figure 5C).

In comparison, the interactions between the adenine and ribose groups of ADP with the enzyme appear to be weaker. The hydroxyls on the ribose have no direct interactions with the enzyme. The adenine base of ADP has amino-aromatic interactions with the side chain of Arg128 (Figure 5B), but is otherwise exposed to solvent (Figure 4B). This Arg residue comes from helix αD in the LID and is present in many of the structurally related kinases.

The conformations of the 16 copies of NRK1 in the crystallographic asymmetric unit, in the ternary complex with

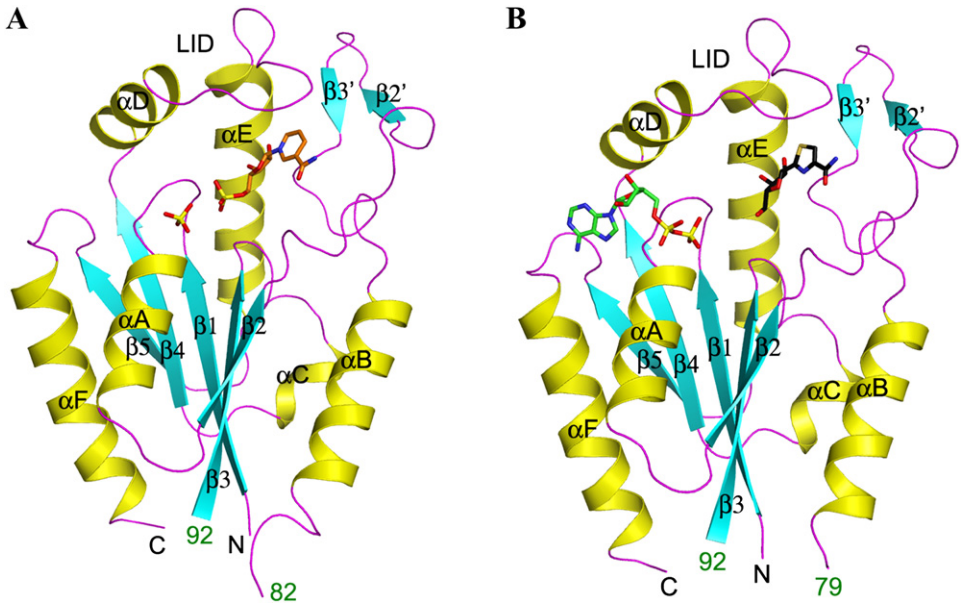

Figure 2. Structure of Human NRK1

(A) Schematic representation of the structure of human NRK1 in a binary complex with reaction product NMN (in orange for carbon atoms).
(B) Structure of human NRK1 in a ternary complex with ADP (green) and tiazofurin (black).
This figure was produced with PyMOL (DeLano, 2002).

ADP and tiazofurin, are essentially identical; there is an rms distance of 0.1 Å among their equivalent Cα atoms. Human NRK1 is monomeric in solution (unpublished data and Sasiak and Saunders, 1996). In comparison, the dNKs are dimeric in solution (Eriksson et al., 2002; Welin et al., 2007). Noncrystallographic symmetry (NCS) restraint was applied in the refinement, but reducing the weight on the NCS restraint did not significantly affect the structures. On the other hand, there are clear structural differences between this ternary complex and the binary complex with NMN. This is especially true for the LID and the αA helix (Figure 5C), which are involved in binding ADP. In comparison, the central β sheet has few structural differences in the two complexes. The rms distance among 176 equivalent Cα atoms of the 2 structures is 0.67 Å.

Implications for Catalysis by NRK

Our structures of the binary complex with NMN and the ternary complex with ADP and tiazofurin provide significant

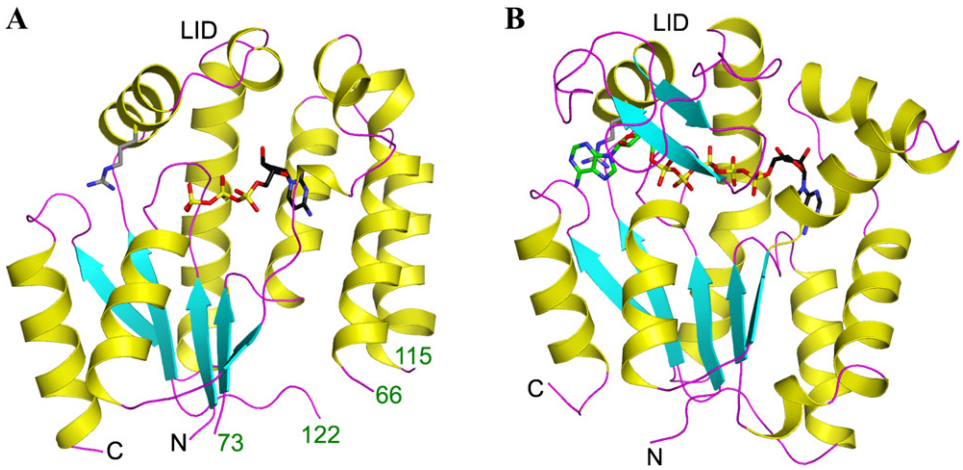

Figure 3. Structural Homologs of NRK1

(A) Schematic representation of the structure of *M. mycoides* deoxyadenosine kinase in complex with dCTP (Welin et al., 2007).
(B) Schematic representation of the structure of yeast adenylate kinase in complex with Ap5A (Abele and Schulz, 1995).
This figure was produced with PyMOL (DeLano, 2002).

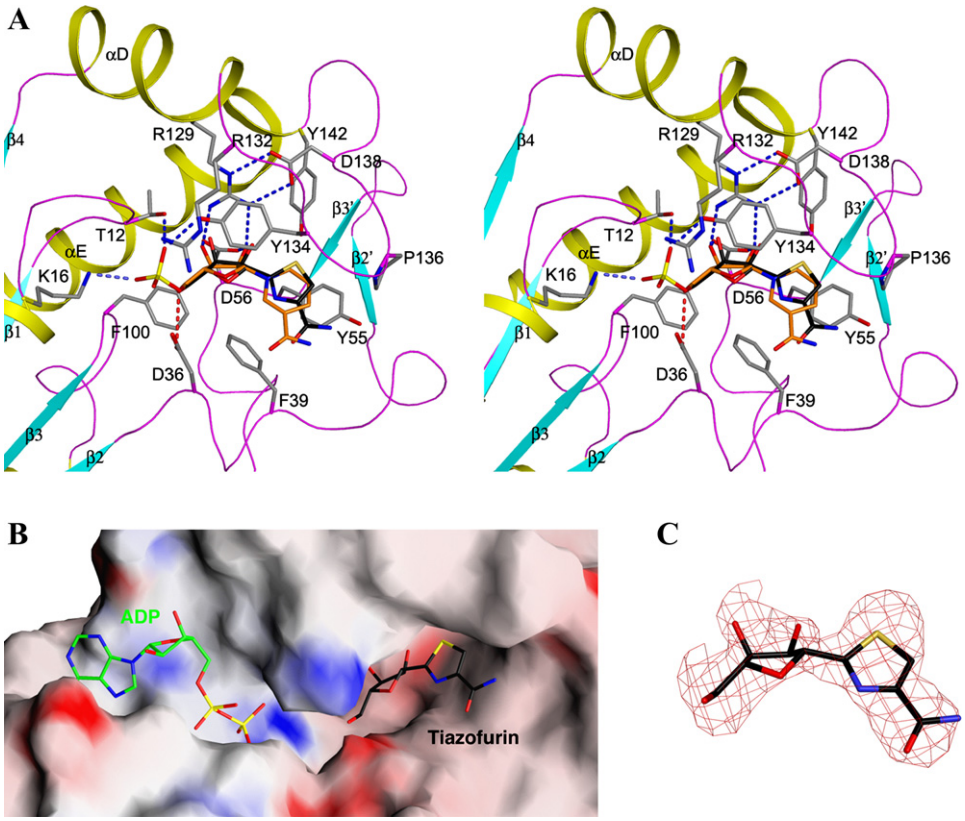

Figure 4. The Binding Modes of NMN and Tiazofurin

(A) The binding site for NMN. Hydrogen-bonding interactions are indicated with blue, dashed lines. The binding mode of tiazofurin is also shown (in black).

(B) Molecular surface of the active-site region of NRK1, colored based on electrostatic potential.

(C) Final $2F_o - F_c$ electron density for tiazofurin at 2.7 Å resolution. Contoured at 1σ.

(A) and (C) were produced with PyMOL (DeLano, 2002); (B) was produced with Grasp (Nicholls et al., 1991).

insights into the catalysis by NRK. The structural information allowed us to produce a model for the enzyme in complex with its substrates ATP and NR (Figure 6A), as well as with its products ADP and NMN (Figure 6B). The structural analysis suggests that Asp36 is the general base of the enzyme, extracting the proton from the 5′ hydroxyl of the NR substrate. In the model, this hydroxyl is only 3.4 Å from the γ-phosphorus atom in ATP and is in the correct position to initiate nucleophilic attack on this phosphate. The distance between the γ-phosphate group of ATP and the phosphate group in NMN is 1.7 Å, suggesting that only a relatively small movement is needed for the phospho-transfer reaction. The structures show that the nicotinamide group is not recognized specifically by the enzyme, suggesting that NRK could be active with other phospho-acceptors, as has been observed with tiazofurin and other nucleosides (Bieganowski and Brenner, 2004; Sasiak and Saunders, 1996).

Mutagenesis Studies Confirm the Structural Observations

To assess the information obtained from the structures, we selected several residues that appear to play important roles in substrate binding and/or catalysis and characterized their functional importance by mutagenesis experiments. The kinetic assay converts the NMN product to NADH, through the coupling enzymes NMNAT and alcohol dehydrogenase (Khan et al., 2006; Revollo et al., 2004). The substrate NR was produced by dephosphorylation of NMN (Bieganowski and Brenner, 2004). The assays showed that human NRK1 has robust catalytic activity toward the NR substrate, which has a K_M of about 3.7 μM (Figure 7A) (Sasiak and Saunders, 1996).

Mutation of the catalytic base, Asp36, essentially abolished the activity of the enzyme (Figure 7B). Similarly, mutations of Asp56, which has an important role in recognizing the ribose hydroxyls of NR, and Lys16 in the P loop, which is crucial for ATP binding, also inactivated the enzyme. In comparison, mutation of Asp138, ion paired to Arg129 that is hydrogen bonded to the ribose hydroxyls, has only minor effects on catalysis by the enzyme (Figure 7B). Overall, our structural observations are confirmed by the mutagenesis and kinetic studies.

In summary, we have determined the crystal structures of human NRK1 in a binary complex with its product NMN and in a ternary complex with ADP and the anticancer

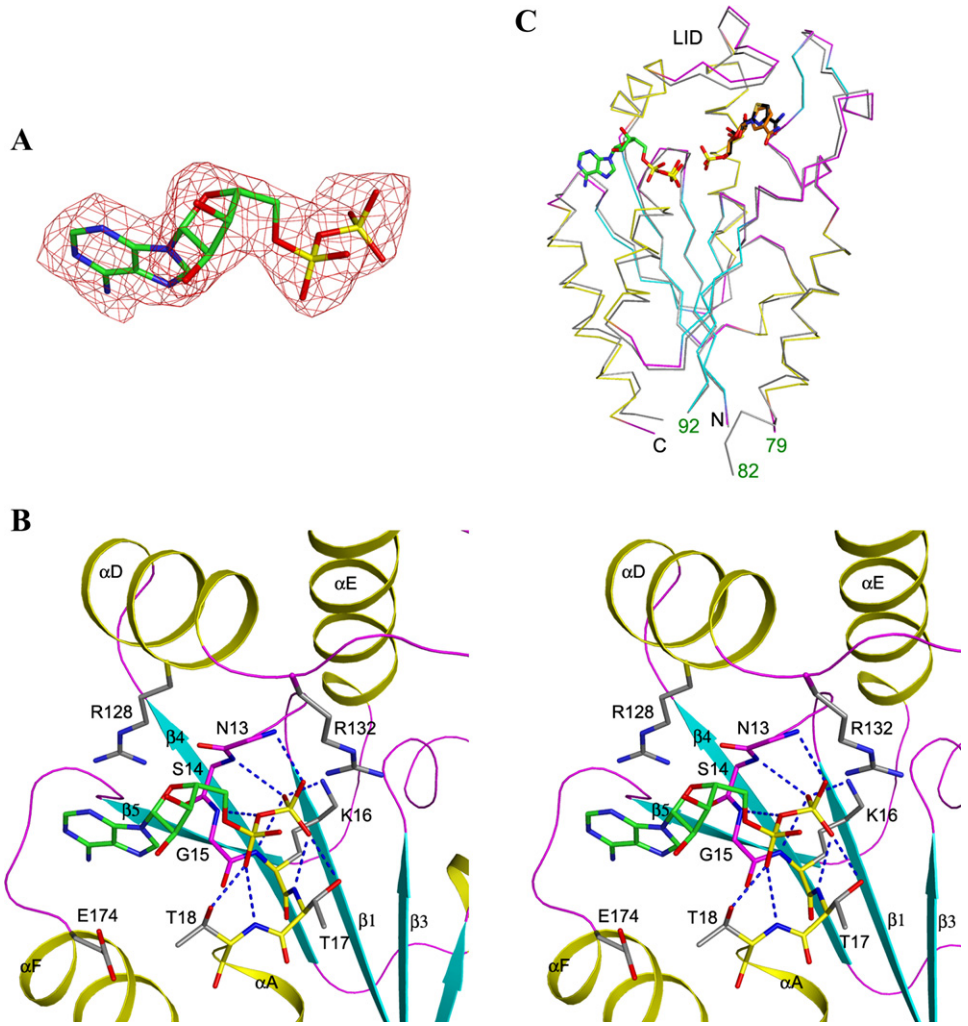

Figure 5. The Binding Mode of ADP

(A) Final $2F_o - F_c$ electron density for ADP at 2.7 Å resolution. Contoured at 1σ.

(B) The binding site for ADP. Hydrogen-bonding interactions are indicated with blue, dashed lines.

(C) Overlay of the structures of the binary complex with NMN (in gray) and the ternary complex with ADP:tiazofurin.

This figure was produced with PyMOL (DeLano, 2002).

drug tiazofurin. The structures reveal a unique conformation for the NMP-binding domain, distinct from those in the other enzymes of this superfamily. The structural information also provides significant insight into the catalysis by this enzyme, which has been confirmed by our mutagenesis experiments.

EXPERIMENTAL PROCEDURES

Protein Expression and Purification

Full-length human NRK1 (residues 1–199) was subcloned into the pET24d vector (Novagen) and overexpressed in *Escherichia coli* at 20°C. The expression construct introduced a hexahistidine tag at the C terminus. The soluble protein was purified by nickel-agarose affinity chromatography, anion-exchange chromatography, and gel-filtration chromatography. The protein was concentrated to 40 mg/ml in a buffer containing 20 mM Tris (pH 7.5), 200 mM NaCl, 5 mM DTT, and 5% (v/v) glycerol and was stored at −80°C.

The selenomethionyl protein sample was produced in minimal media supplemented with specific amino acids to inhibit endogenous methionine biosynthesis (Doublie et al., 1996) and was purified by following the same protocol as that used for the native enzyme.

Protein Crystallization

Crystals of selenomethionyl NRK1 in complex with NMN were obtained at 22°C with the sitting-drop vapor-diffusion method. The protein at 20 mg/ml concentration was incubated with 2 mM NMN (protein:NMN molar ratio of 1:2) at 4°C for 30 min before setting up crystal trays. The reservoir solution contained 28% (w/v) PEG 3350, 200 mM NH_4Cl, 5 mM DTT, and 5 mM Na_2HPO_4. The crystals were cryoprotected by transfer to the reservoir solution supplemented with 5% (v/v) glycerol and were flash frozen in liquid propane for data collection at 100 K. They belong to space group $C222_1$, with cell parameters of a = 54.72 Å, b = 141.53 Å, and c = 62.09 Å. There is one molecule of NRK1 in the asymmetric unit.

Crystals of NRK1 in complex with tiazofurin and ADP were obtained under similar conditions as those for the NMN complex. The protein (20 mg/ml) was incubated with 2 mM tiazofurin and 2 mM ADP

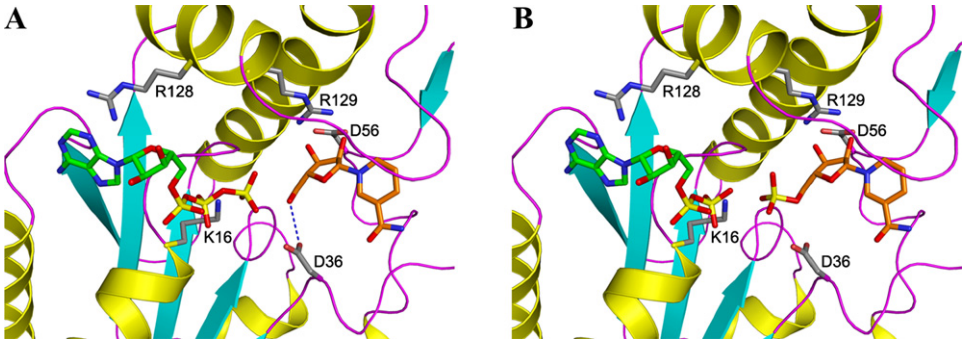

Figure 6. Models for the Substrate and Product Complexes of NRK1
(A) Model of NRK1 in a ternary complex with the substrates ATP and NR. Asp36 is the general base that extracts the proton from NR.
(B) Model of NRK1 in a ternary complex with the products ADP and NMN.
This figure was produced with PyMOL (DeLano, 2002).

(protein:ligand molar ratio of 1:2) at 4°C for 30 min before setting up trays. The pH of the ADP solution was adjusted to 7.8. The crystals were washed once with the reservoir solution supplemented with 2 mM tiazofurin and 2 mM ADP and were flash cooled in liquid nitrogen. They belong to space group $P2_1$, with cell parameters of a = 145.71 Å, b = 99.96 Å, c = 145.59 Å and β = 91.57°. There are 16 NRK1 monomers in the asymmetric unit.

Data Collection and Processing

A selenomethionyl SAD data set at 1.5 Å resolution was collected at 100 K on the NMN complex at the X4A beamline of Brookhaven National Laboratory. A native reflection data set was collected for the ADP:tiazofurin complex at the X29 beamline. The diffraction images were processed and scaled with the HKL package (Otwinowski and Minor, 1997). The data processing statistics are summarized in Table 1.

Structure Determination and Refinement

For the NMN complex, the locations of the selenomethionyl atoms were determined with the program BnP (Weeks and Miller, 1999). Reflection phases to 1.5 Å resolution were calculated based on the SAD data and were improved with the program SOLVE/RESOLVE (Terwilliger, 2003), which also automatically located most of the residues. The complete atomic model was fit into the electron density with the program O (Jones et al., 1991). The structure refinement was carried out with the program CNS (Brunger et al., 1998). The refinement statistics are summarized in Table 1.

Crystals of the ADP:tiazofurin complex were microscopically twinned, possibly due to the fact that the a and c axes of the unit cell are almost identical, and that the β angle is close to 90°. A twinning fraction of 0.37 was estimated by CNS, by simulating the hemihedral twinning case of P4. The structure was solved by molecular replacement with the program Phaser (Storoni et al., 2004). Twinned refinement was carried out with CNS, with the twinning operator $l - k\,h$. Noncrystallographic symmetry restraints were applied to the 16 NRK1 molecules in the asymmetric unit.

Mutagenesis

Mutants of NRK1 were designed based on the structural information, created with the QuikChange kit (Stratagene), and sequenced to confirm the incorporation of the correct mutation. The mutant proteins were purified by following the same protocol as that used for the wild-type enzyme.

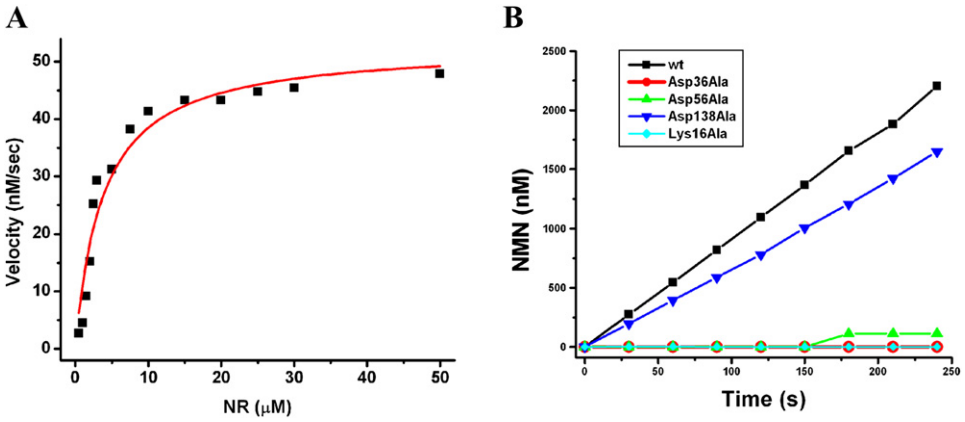

Figure 7. Mutagenesis Studies Confirm the Structural Observations
(A) Purified NRK1 has robust activity toward the NR substrate. The experimental data (black squares) were fitted to the Michaelis-Menten equation (red curve) by nonlinear regression, defining the K_M and V_{max} values. The assay followed the production of NADH, through the coupling enzymes NMNAT and alcohol dehydrogenase (Bieganowski and Brenner, 2004; Khan et al., 2006; Revollo et al., 2004). Data from one representative experiment of several different repeats are shown.
(B) Mutations in the active-site region can abolish the catalytic activity. The mutants were designed based on the structural information, and their effects on catalysis were determined by the kinetic assay.

NRK Assays

The substrate nicotinamide riboside (NR) was generated by following a published protocol (Bieganowski and Brenner, 2004), by treating NMN with calf intestinal alkaline phosphatase (CIP) at 37°C overnight. A typical reaction contained 20 mM Tris (pH 7.9), 100 mM NaCl, 5 mM $MgCl_2$, 100 mM NMN (Sigma), and 1500 U CIP (New England Biolabs) in a volume of 0.5 ml. The NR was separated from CIP by centrifugation through a 10 kDa filter (Millipore). The quality of this substrate was analyzed by the NRK1 assay described below, except that the NRK1 enzyme was omitted from the reaction mixture. Typically, no visible contamination by NMN was detected even when the substrate was used at high concentrations (~20 mM).

All of the assays were repeated several times to ensure the reproducibility of the experiments. The catalytic activity of NRK1 was determined by using a coupled enzyme spectrometric assay. Briefly, the NMN product of NRK was converted to NAD^+ with the enzyme NMN/NAMN adenylyltransferase (NMNAT), and NAD^+ was then reduced to NADH by alcohol dehydrogenase (Sigma) by using ethanol as the substrate (Khan et al., 2006; Revollo et al., 2004). By monitoring the appearance of NADH at 340 nm, the activity of NRK could be determined. Human NMNAT was overexpressed in *E. coli* and was purified by following a published protocol (Zhou et al., 2002). The reaction buffer contained 50 mM Tris (pH 7.5), 100 mM NaCl, various concentrations of NR, 2.5 mM ATP, 12 mM $MgCl_2$, 1.5% (v/v) ethanol, 10 mM semicarbazide (to remove the acetaldehyde product of ethanol oxidation), 0.02% (w/v) BSA, 10 μg/ml NMNAT, 30 μg/ml alcohol dehydrogenase, and 0.2 μM NRK. The reactions are carried out at room temperature. For the mutants, the reactions were monitored at 25 μM substrate concentration.

ACKNOWLEDGMENTS

We thank Victor Marquez at the National Cancer Institute for the gift of tiazofurin, Todd Yeates for helpful discussions about twinning, Randy Abramowitz and John Schwanof for setting up the X4A beamline, and Howard Robinson and Wuxian Shi for setting up the X29 beamline at the National Synchrotron Light Source. This research is supported in part by a grant from the National Institutes of Health to L.T.

Received: May 5, 2007
Revised: June 13, 2007
Accepted: June 27, 2007
Published: August 14, 2007

REFERENCES

Abele, U., and Schulz, G.E. (1995). High-resolution structures of adenylate kinase from yeast ligated with inhibitor Ap5A, showing the pathway of phosphoryl transfer. Protein Sci. *4*, 1262–1271.

Appleby, T.C., Larson, G., Cheney, I.W., Walker, H., Wu, J.Z., Zhong, W., Hong, Z., and Yao, N. (2005). Structure of human uridine-cytidine kinase 2 determined by SIRAS using a rotating-anode X-ray generator and a single samarium derivative. Acta Crystallogr. D Biol. Crystallogr. *61*, 278–284.

Berger, F., Ramirez-Hernandez, M.H., and Ziegler, M. (2004). The new life of a centenarian: signaling functions of NAD(P). Trends Biochem. Sci. *29*, 111–118.

Bieganowski, P., and Brenner, C. (2004). Discoveries of nicotinamide riboside as a nutrient and conserved NRK genes establish a Preiss-Handler independent route to NAD^+ in fungi and humans. Cell *117*, 495–502.

Blander, G., and Guarente, L. (2004). The Sir2 family of protein deacetylases. Annu. Rev. Biochem. *73*, 417–435.

Brunger, A.T., Adams, P.D., Clore, G.M., DeLano, W.L., Gros, P., Grosse-Kunstleve, R.W., Jiang, J.-S., Kuszewski, J., Nilges, M., Pannu, N.S., et al. (1998). Crystallography & NMR System: a new software suite for macromolecular structure determination. Acta Crystallogr. *D54*, 905–921.

DeLano, W.L. (2002). The PyMOL Molecular Graphic System (San Carlos, CA: DeLano Scientific).

Denu, J.M. (2005). The Sir2 family of protein deacetylases. Curr. Opin. Chem. Biol. *9*, 431–440.

Doublie, S., Kapp, U., Aberg, A., Brown, K., Strub, K., and Cusack, S. (1996). Crystallization and preliminary X-ray analysis of the 9 kDa protein of the mouse signal recognition particle and the selenomethionyl-SRP9. FEBS Lett. *384*, 219–221.

Eriksson, S., Munch-Petersen, B., Johansson, K., and Eklund, H. (2002). Structure and function of cellular deoxyribonucleoside kinases. Cell. Mol. Life Sci. *59*, 1327–1346.

Grifantini, M. (2000). Tiazofurine ICN pharmaceuticals. Curr. Opin. Investig. Drugs *1*, 257–262.

Guse, A.H. (2005). Second messenger function and the structure-activity relationship of cyclic adenosine diphosphoribose (cADPR). FEBS J. *272*, 4590–4597.

Hartmann, M.D., Bourenkov, G.P., Oberschall, A., Strizhov, N., and Bartunik, H.D. (2006). Mechanism of phosphoryl transfer catalyzed by shikimate kinase from *Mycobacterium tuberculosis*. J. Mol. Biol. *364*, 411–423.

Hasmann, M., and Schemainda, I. (2003). FK866, a highly specific non-competitive inhibitor of nicotinamide phosphoribosyltransferase, represents a novel mechanism for induction of tumor cell apoptosis. Cancer Res. *63*, 7436–7442.

Hendrickson, W.A. (1991). Determination of macromolecular structures from anomalous diffraction of synchrotron radiation. Science *254*, 51–58.

Holm, L., and Sander, C. (1993). Protein structure comparison by alignment of distance matrices. J. Mol. Biol. *233*, 123–138.

Izard, T., and Ellis, J. (2000). The crystal structures of chloramphenicol phosphotransferase reveal a novel inactivation mechanism. EMBO J. *19*, 2690–2700.

Jager, W., Salamon, A., and Szekeres, T. (2002). Metabolism of the novel IMP dehydrogenase inhibitor benzamide riboside. Curr. Med. Chem. *9*, 781–786.

Jauch, R., Humm, A., Huber, R., and Wahl, M.C. (2005). Structures of *Escherichia coli* NAD synthetase with substrates and products reveal mechanistic rearrangements. J. Biol. Chem. *280*, 15131–15140.

Jones, T.A., Zou, J.Y., Cowan, S.W., and Kjeldgaard, M. (1991). Improved methods for building protein models in electron density maps and the location of errors in these models. Acta Crystallogr. A *47*, 110–119.

Khan, J.A., Tao, X., and Tong, L. (2006). Molecular basis for the inhibition of human NMPRTase, a novel target for anticancer agents. Nat. Struct. Mol. Biol. *13*, 582–588.

Khan, J.A., Forouhar, F., Tao, X., and Tong, L. (2007). Nicotinamide adenine dinucleotide metabolism as attractive target for drug discovery. Expert Opin. Ther. Targets *11*, 695–705.

Kraft, L., Sprenger, G.A., and Lindqvist, Y. (2002). Conformational changes during the catalytic cycle of gluconate kinase as revealed by X-ray crystallography. J. Mol. Biol. *318*, 1057–1069.

Lavie, A., Konrad, M., Brundiers, R., Goody, R.S., Schlichting, I., and Reinstein, J. (1998a). Crystal structure of yeast thymidylate kinase complexed with the bisubstrate inhibitor P1-(5′-adenosyl) P5-(5′-thymidyl) pentaphosphate (TP5A) at 2.0 Å resolution: implications for catalysis and AZT activation. Biochemistry *37*, 3677–3686.

Lavie, A., Ostermann, N., Brundiers, R., Goody, R.S., Reinstein, J., Konrad, D., and Schlichting, I. (1998b). Structural basis for efficient phosphorylation of 3′-azidothymidine monophosphate by *Escherichia coli* thymidylate kinase. Proc. Natl. Acad. Sci. USA *95*, 14045–14050.

Lee, H.C. (2004). Multiplicity of Ca^{2+} messengers and Ca^{2+} stores: a perspective from cyclic ADP-ribose and NAADP. Curr. Mol. Med. *4*, 227–237.

Li, F., Chong, Z.Z., and Maiese, K. (2006). Cell life versus cell longevity: the mysteries surrounding the NAD^+ precursor nicotinamide. Curr. Med. Chem. *13*, 883–895.

Magni, G., Amici, A., Emanuelli, M., Raffaelli, N., and Ruggieri, S. (1999). Enzymology of NAD^+ synthesis. Adv. Enzymol. Relat. Areas Mol. Biol. *73*, 135–182.

Magni, G., Amici, A., Emanuelli, M., Orsomando, G., Raffaelli, N., and Ruggieri, S. (2004a). Enzymology of NAD^+ homeostasis in man. Cell. Mol. Life Sci. *61*, 19–34.

Magni, G., Amici, A., Emanuelli, M., Orsomando, G., Raffaelli, N., and Ruggieri, S. (2004b). Structure and function of nicotinamide mononucleotide adenylyltransferase. Curr. Med. Chem. *11*, 873–885.

Nicholls, A., Sharp, K.A., and Honig, B. (1991). Protein folding and association: insights from the interfacial and thermodynamic properties of hydrocarbons. Proteins *11*, 281–296.

Otwinowski, Z., and Minor, W. (1997). Processing of X-ray diffraction data collected in oscillation mode. Methods Enzymol. *276*, 307–326.

Pankiwicz, K.W., Patterson, S.E., Black, P.L., Jayaram, H.N., Risal, D., Goldstein, B.M., Stuyver, L.J., and Schinazi, R.F. (2004). Cofactor mimics as selective inhibitors of NAD-dependent inosine monophosphate dehydrogenase (IMPDH)-the major therapeutic target. Curr. Med. Chem. *11*, 887–900.

Revollo, J.R., Grimm, A.A., and Imai, S.-I. (2004). The NAD biosynthesis pathway mediated by nicotinamide phosphoribosyltransferase regulates Sir2 activity in mammalian cells. J. Biol. Chem. *279*, 50754–50763.

Revollo, J.R., Grimm, A.A., and Imai, S. (2007). The regulation of nicotinamide dinucleotide biosynthesis by Nampt/PBEF/visfatin in mammals. Curr. Opin. Gastroenterol. *23*, 164–170.

Rizzi, M., Nessi, C., Mattevi, A., Coda, A., Bolognesi, M., and Galizzi, A. (1996). Crystal structure of NH_3-dependent NAD^+ synthetase from *Bacillus subtilis*. EMBO J. *15*, 5125–5134.

Rongvaux, A., Andris, F., van Gool, F., and Leo, O. (2003). Reconstructing eukaryotic NAD metabolism. Bioessays *25*, 683–690.

Sasiak, K., and Saunders, P.P. (1996). Purification and properties of a human nicotinamide ribonucleotide kinase. Arch. Biochem. Biophys. *333*, 414–418.

Schreiber, V., Dantzer, F., Ame, J.C., and de Murcia, G. (2006). Poly-(ADP-ribose): novel functions for an old molecule. Nat. Rev. Mol. Cell Biol. *7*, 517–528.

Stehle, T., and Schulz, G.E. (1992). Refined structure of the complex between guanylate kinase and its substrate GMP at 2.0 Å resolution. J. Mol. Biol. *224*, 1127–1141.

Storoni, L.C., McCoy, A.J., and Read, R.J. (2004). Likelihood-enhanced fast rotation functions. Acta Crystallogr. D Biol. Crystallogr. *60*, 432–438.

Terwilliger, T.C. (2003). SOLVE and RESOLVE: automated structure solution and density modification. Methods Enzymol. *374*, 22–37.

Weeks, C.M., and Miller, R. (1999). The design and implementation of SnB v2.0. J. Appl. Cryst. *32*, 120–124.

Welin, M., Wang, L., Eriksson, S., and Eklund, H. (2007). Structure-function analysis of a bacterial deoxyadenosine kinase reveals the basis for substrate specificity. J. Mol. Biol. *366*, 1615–1623.

Wojcik, M., Seidle, H.F., Bieganowski, P., and Brenner, C. (2006). Glutamine-dependent NAD^+ synthetase. How a two-domain, three-substrate enzyme avoids waste. J. Biol. Chem. *281*, 33395–33402.

Yan, H., and Tsai, M.D. (1999). Nucleoside monophosphate kinases: structure, mechanism, and substrate specificity. Adv. Enzymol. Relat. Areas Mol. Biol. *73*, 103–134.

Ying, W. (2006). NAD^+ and NADH in cellular functions and cell death. Front. Biosci. *11*, 3129–3148.

Yun, M., Park, C.-G., Kim, J.-Y., Rock, C.O., Jackowski, S., and Park, H.-W. (2000). Structural basis for the feedback regulation of *Escherichia coli* pantothenate kinase by coenzyme A. J. Biol. Chem. *275*, 28093–28099.

Zhou, T., Kurnasov, O., Tomchick, D.R., Binns, D.D., Grishin, N.V., Marquez, V.E., Osterman, A.L., and Zhang, H. (2002). Structure of human nicotinamide/nicotinic acid mononucleotide adenylyltransferase. Basis for the dual substrate specificity and activation of the oncolytic agent tiazofurin. J. Biol. Chem. *277*, 13148–13154.

Accession Numbers

Coordinates have been deposited in the Protein Data Bank with accession codes 2QG6 and 2QL6.